Rigorous Analysis of 3-D Planar Circuit Discontinuities Using the Space-Spectral Domain Approach (SSDA)

Ke Wu, *Member, IEEE,* Ming Yu, *Student Member, IEEE,* and Ruediger Vahldieck, *Senior Member, IEEE*

***Abstract*—A new method, the Space-Spectral Domain Approach (SSDA), has been developed to determine scattering parameters for arbitrarily shaped multilayered planar MIC/MMIC discontinuities. Although the basic framework of the SSDA has been introduced previously, only resonant frequencies of planar circuit discontinuities could be calculated. The SSDA as presented in this paper is not only significantly extended, but it also introduces the new concept of self-consistent hybrid boundary conditions to replace the modal source concept in the feed line. Furthermore, a general error function is derived to provide a direct assessment of the discretization accuracy. The convergence behavior of this new method is investigated, and current standing-wave profiles along microstrip throughlines with matched, open and short-circuited conditions are given. Finally, *S*-parameters for several microstrip discontinuities with abrupt and smooth transition are illustrated to demonstrate the flexibility of this new approach.**

Introduction

ACCURATE characterization of planar discontinuities is the basis for industrial applications of computer-aided design of monolithic microwave integrated circuits (MMIC) and miniature hybrid microwave integrated circuits (MHMIC). In general, these circuits are composed of cascaded planar transmission lines which are interconnected by circuit discontinuities. The difficulties in describing the scattering parameters of these discontinuities are accentuated by the possibility of an irregularly shaped contour and the presence of a multilayered substrate topology.

Hitherto known full-wave techniques applicable to arbitrarily shaped 3-D discontinuities are mostly based on spatial discretization of the structure (i.e., FDTD [1]–[2], TLM [3], [4], FEM [5], [6]). Although these techniques are very flexible, they provide accurate results only at the expense of memory space and CPU time. This is in particular true when very thin substrate layers are involved (i.e., insulating layers in semiconductor based transmission lines). In this case, techniques which also discretize the space transverse to the propagation direction need a very fine resolution to accommodate these layers. This may require the use of supercomputer power to obtain results in a reasonable time. Other techniques which are known to be computationally very efficient, like the spectral domain approach (SDA) [7]–[9] and other alternative methods [10]–[12], lose some of their advantages when applied to spatial 3-D discontinuities. In particular when these discontinuities are arbitrarily shaped, convergence of the basis functions (SDA) becomes generally a problem.

To avoid difficulties associated with 2-D basis functions or 3-D spatial discretization, the authors recently [18], [19] have introduced a novel combination of two different modeling techniques, the method of lines (MOL) [13]–[16] and the SDA, to form the space spectral domain approach (SSDA). In this technique, the disadvantages associated with each of the methods when applied individually to 3-D discontinuities can be largely eliminated. This is so, because the MOL is most efficient when only one spatial variable needs to be discretized and similarly, the SDA is most efficient when only 1-D basis functions are used. Therefore, the SSDA combines the 1-D SDA (which is used to describe only the plane transverse to the propagation direction) with the 1-D MOL (which describes the circuit in propagation direction). This combination takes advantage of the flexibility of the MOL to model arbitrary discontinuities and at the same time adds the computational efficiency of the SDA. In addition, the SSDA accounts automatically for the singularity of fields (or currents) along the edges of slots (or strips).

So far the SSDA has only been capable of analyzing resonant structures. In this paper the SSDA is extended to calculate the s-parameters of discontinuities. This extended version of the SSDA employs the concept of self-consistent inhomogeneous (or hybrid) boundary conditions at the end of feedlines which are connected to either side of the discontinuity.

This approach makes it possible to simulate the whole structure via an eigenvalue equation in which the solution

Manuscript received August 19, 1991; revised February 12, 1992. This work was supported by Microtel Pacific Research Ltd. (MPR), Vancouver, and the Natural Sciences and Engineering Research Council (NSERC) of Canada.

K. Wu was with the Department of Electrical and Computer Engineering, University of Victoria, P.O. Box 3055, Victoria, BC, Canada V8W 3P6. He is presently with the Département de génie électrique École Polytechnique, Case postale 6079, succursale A. Montréal, PQ, Canada H3C 3A7.

M. Yu and R. Vahldieck are with the Department of Electrical and Computer Engineering, University of Victoria, P.O. Box 3055, Victoria, BC, Canada V8W 3P6.

IEEE Log Number 9108319.

is the reflection coefficient of the discontinuity. The hybrid boundary conditions have been used before in [21] and [22] but in the first case to model the forward and reflected waves individually and in the second case to find the total field at the launching point by using a modal source approach. In the method presented here, the reflection coefficient (or s_{11}) is obtained directly.

Another contribution resulting from this work is that error functions are derived based on a comparison between the differential and difference operators in the inhomogeneous boundary conditions. These functions are useful in determining the discretization accuracy and the error introduced. At the same time, a limiting criterion is derived which indicates when and how the discretization size should be changed.

Theory

In the following the equidistant discretization scheme is used for simplicity. The scattering parameter analysis of a 3-D planar discontinuity problem with arbitrary contour and multilayered substrates is shown in Fig. 1. The electromagnetic field in each dielectric region is described by two scalar potential functions, ψ^e and ψ^h, which satisfy the Helmholtz equation and the boundary conditions. Both potential functions are z-oriented and hence correspond to the TM and TE modes in the guided structure. Since the principal analytical steps involved in the space-spectral domain approach have been well explained in [19], the emphasis in the following analysis is on how to simulate the 3-D scattering problems by the self-consistent inhomogeneous boundary conditions implemented in the SSDA algorithm.

Instead of discretizing the 3-D planar structure in the x and z directions as required by the conventional 2-D MOL, the structure is discretized in the z-direction only. This step corresponds to slicing the structure in the x-y planes for each of the two scalar potential functions separately. The distance between two slices is determined by the discretization size h. Using the Fourier transform, the two scalar potential functions are written in the spectral domain along the x-direction. This step means that a set of continuous expansion functions are assigned to each discrete line. Considering a structure with open bilateral boundaries leads to infinite integrals, these can be approximated by the integration over a finite space $(0, a)$ [23]:

$$\tilde{\psi}^{e,h}(\alpha, y, z) = \int_{-\infty}^{+\infty} \psi^{e,h}(x,y,z)e^{j\alpha x}\,dx \approx \int_0^a \psi^{e,h}(x,y,z)e^{j\alpha x}\,dx. \quad (1)$$

A. Inhomogeneous (Hybrid) Boundary Conditions

It is assumed that at some distance from Port 1 of the discontinuity there will be a standing wave of the fundamental mode only consisting of incident and reflected waves:

$$\psi^e = \psi_0^e(e^{-j\beta_1 z} - re^{j\beta_1 z})$$
$$\psi^h = \psi_0^h(e^{-j\beta_1 z} + re^{j\beta_1 z}) \quad (2)$$

where β_1 is the propagation constant at the boundary of Port 1 calculated separately by using the SDA, r is the voltage reflection coefficient and ψ_0^e, ψ_0^h are the incident TE/TM potentials at $z = 0$. The inhomogeneous boundary conditions can be derived independently without considering the spectral domain factors. With reference to the matched, open- and short-circuited conditions, as illustrated in Fig. 1, three different cases for the boundaries exist, these are the Dirichlet, Neumann and hybrid boundary conditions. For the matched condition at Port 2 there are two choices for the discretization scheme depending on whether to assign an e or h line as the first line. In the following, the discretization scheme begins with an h-line (open-circuit).

In case of the matched and open-circuit conditions, the hybrid boundary condition at $z = 0$ for ψ^e can be expressed as

$$\psi^e|_{z=0} = \psi_1^e \quad \text{(Dirichlet kind)} \quad (3)$$

and at $z = 0.5\,h$ for ψ^h:

$$\left.\frac{\partial \psi^h}{\partial z}\right|_{z=0.5h} = \frac{\partial \psi_1^h}{\partial z} = -j\beta_1 \frac{1 - j\tau tg(0.5\beta_1 h)}{\tau - jtg(0.5\beta_1 h)}\psi_1^h$$

(Neumann kind) (4)

in which $\tau = (1 + r)/(1 - r)$. The voltage reflection coefficient is thus explicitly involved in the hybrid boundary conditions. At Port 2 the matched and open-circuit

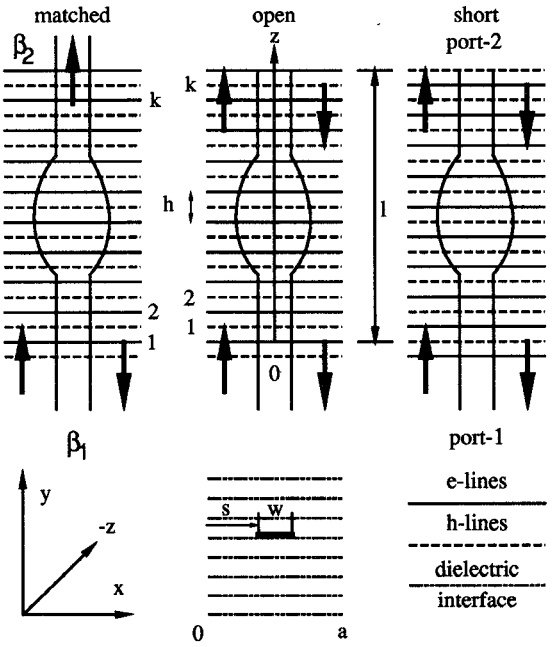

Fig. 1. Illustration of an arbitrary 3-D planar multilayered circuits with matched, open and short circuited Port 2.

conditions correspond to:

$$\left.\frac{\partial \psi^e}{\partial z}\right|_{z=L-h} = \frac{\partial \psi_k^e}{\partial z} = -j\beta_2 \psi_k^e$$

(matched condition) (5)

and

$$\left.\frac{\partial \psi^e}{\partial z}\right|_{z=L-h} = \frac{\partial \psi_k^e}{\partial z} \approx \frac{\Delta \psi_k^e}{\Delta z} = -\frac{1}{h}\psi_k^e$$

(open-circuited condition) (6)

respectively, where β_2 is the propagation constant at Port 2 if a two-port circuit is considered. The propagation constants β_1 and β_2 can be derived from the 1-D SDA or MOL. Note that the matched condition corresponds to the discretization scheme of the open-circuit condition. In a similar way, the hybrid boundary conditions obtained for the short-circuit situation is as follows:

$$\left.\frac{\partial \psi^e}{\partial z}\right|_{z=0.5h} = \frac{\partial \psi_1^e}{\partial z} = -j\beta_1 \frac{\tau - jtg(0.5\beta_1 h)}{1 - j\tau tg(0.5\beta_1 h)}\psi_1^e$$

(at Port 1)

$$\left.\frac{\partial \psi^h}{\partial z}\right|_{z=L-h} = \frac{\partial \psi_k^h}{\partial z} \approx \frac{\Delta \psi_k^h}{\Delta z} = -\frac{1}{h}\psi_k^h$$

(at Port-2) (7)

Obviously, the potential functions and their first derivatives constitute the characteristic solutions of the whole circuit. It is interesting to see that the complex functions of the inhomogeneous boundary conditions at the input described in (4) and (7) are not only expressed in terms of the propagation constant β_1, but also the discretization interval h and the unknown voltage reflection coefficient r (or s_{11}). In other words, the inhomogeneous boundary conditions are no longer "static" and strongly depend on the unknown scattering parameter, which in turn depends on the geometry of the structure of interest as well as the operating frequency. This is why the inhomogeneous boundary conditions are said to be self-consistent.

B. Error Functions and Limiting Conditions of Discretization

Judging from the inhomogeneous boundary conditions, the discretization size h is involved and plays an important role in the analysis. Intuitively speaking, the smaller the interval h is, the more accurate the numerical results become. However, it is not advisable to chose a very fine discretization scheme since this leads not only to a time-consuming algorithm but also deteriorates its efficiency and stability. So far, there is no detailed analysis treating this problem. In the following, analytical error functions are introduced to provide some criteria on the limiting conditions of the discretization. These criteria are useful for gaining insight into the error magnitude introduced in the analysis due to the discretization.

To begin with, the finite difference operator is applied to approximate the differential operator in dealing with the inhomogeneous boundary conditions at both Port 1 and Port 2. In view of the matched or open-circuit condition, as shown in Fig. 1, a simple analytical expression is obtained from (2):

$$\left.\frac{\Delta \psi^h}{\Delta z}\right|_{z=0.5h} = \frac{\psi_1^h - \psi_0^h}{h} = -j\beta_1 \frac{\sin(0.5\beta_1 h)}{0.5\beta_1 h} \cdot \frac{(1-r)}{e^{-j0.5\beta_1 h}} + re^{j0.5\beta_1 h}\psi_1^h. \quad (8)$$

In comparison with (4), the error function at Port 1 can be defined by the difference operator over its differential counterpart:

$$\xi_1 = 1 - \left|\frac{\left.\frac{\Delta \psi^h}{\Delta z}\right|_1}{\left.\frac{\partial \psi^h}{\partial z}\right|_1}\right| \quad (9)$$

with

$$\frac{\left.\frac{\Delta \psi^h}{\Delta z}\right|_1}{\left.\frac{\partial \psi^h}{\partial z}\right|_1} = \frac{tg(0.5\beta_1 h)}{0.5\beta_1 h}\frac{1}{1 - j\tau tg(0.5\beta_1 h)}. \quad (10)$$

Similarly, the error function is obtained for the short-circuit condition, which essentially is the same expression as (10) after replacing τ by $1/\tau$:

$$\xi_1 = 1 - \left|\frac{\left.\frac{\Delta \psi^e}{\Delta z}\right|_1}{\left.\frac{\partial \psi^e}{\partial z}\right|_1}\right| \quad (11)$$

with

$$\frac{\left.\frac{\Delta \psi^e}{\Delta z}\right|_1}{\left.\frac{\partial \psi^e}{\partial z}\right|_1} = \frac{tg(0.5\beta_1 h)}{0.5\beta_1 h}\frac{\tau}{\tau - jtg(0.5\beta_1 h)}. \quad (12)$$

The error function at Port 2 can also be derived based on the same definition as in (9) and (11) if the matched condition is considered:

$$\xi_2 = 1 - \left|\frac{\left.\frac{\Delta \psi^e}{\Delta z}\right|_k}{\left.\frac{\partial \psi^e}{\partial z}\right|_k}\right| \quad (13)$$

with

$$\left.\frac{\Delta\psi^e}{\Delta z}\right|_k \Big/ \left.\frac{\partial\psi^e}{\partial z}\right|_k = \frac{\sin(0.5\beta_2 h)}{0.5\beta_2 h} e^{-j0.5\beta_2 h}. \tag{14}$$

Apparently, the error functions described in (9)–(14) have the same characteristic behavior as the function $\sin(x)/x$. The minimum point of the error function requires that $x(=\beta h)$ be equal to zero which is impossible in practical applications. Therefore, an error term is inevitably introduced into the analysis. As indicated in (10), (12), and (14), the error function may consist of magnitude and phase, but only the magnitude part is considered here for brevity. Note that although the error function is seemingly defined only at the input, it is virtually valid throughout the line as long as the discretization and fundamental mode are concerned. This is because the differential operations of Maxwell's and Helmholtz' equations are approximated by the corresponding finite difference operation at any location of the line. In general, minimizing the error function is to restrict the product $x(=\beta h)$ within a certain margin close to zero such that the function $\sin(x)/x$ approaches unity. To do so, the following special criteria (3 dB criterion) can be defined:

$$\frac{\sin(0.5\beta h)}{0.5\beta h} \geq 0.707. \tag{15}$$

This is the limiting condition of the discretization, in which β should be $\max(\beta_1, \beta_2)$. Solving (15) leads to the following expression:

$$\frac{h}{\lambda_g} \leq 0.22 \tag{16}$$

where λ_g is the smallest guiding wavelength along the line, Equations (15) and (16) mean that the interval size h should be smaller than one fifth of the guiding wavelength. Although there is no lower limit of the discretization steps, an adequate choice should be made to guarantee both accuracy and efficiency of the algorithm. In view of the required accuracy in practical applications, it is necessary to choose at least one tenth of the guiding wavelength. On the other hand, the error functions defined at Port 1 are dependent on the unknown voltage reflection coefficient, and subsequently on the structure itself. It is believed that such a criterion is not limited to the present method and is also applicable to other approaches employing discretization like TLM, finite-difference technique and even FEM.

C. The Space-Spectral Domain Approach and the Determinant Equation

This section describes the determinant equation derived from the SSDA procedure. The solution of this determinant equation is the unknown reflection coefficient r. The matched condition is taken as an example in the following analysis. The inhomogeneous boundary conditions are

$$\left.\frac{\partial\psi^h}{\partial z}\right|_{z=0.5h} = u\psi_1^h$$
$$\left.\frac{\partial\psi^e}{\partial z}\right|_{z=L-h} = -v\psi_k^e \tag{17}$$

in which u and v are the coefficients defined in (4) and (5). In order to maintain the essential transformation properties (known from the MOL procedure), symmetric second-order finite-difference operators are required to deal with the Helmholtz equation and, in particular, the field equations tangential to the interfaces. Using the concept and algorithm described in [21], the electric and magnetic potential vectors in the original discrete domain are normalized by quasi-complex diagonal matrices [15]–[17]:

$$\bar{\psi}^e = \bar{\bar{r}}^e\bar{\phi}^e$$
$$\bar{\psi}^h = \bar{\bar{r}}^h\bar{\phi}^h \tag{18}$$

with

$$\bar{\bar{r}}^e = \begin{bmatrix} \sqrt{uh} & & & \\ & 1 & & \\ & & \ddots & \\ & & & 1 \end{bmatrix} \tag{19a}$$

$$\bar{\bar{r}}^h = \begin{bmatrix} 1 & & & \\ & \ddots & & \\ & & 1 & \\ & & & \sqrt{vh} \end{bmatrix}. \tag{19b}$$

Therefore, the first derivatives of the potential functions are approximated by

$$\bar{\bar{r}}^{h-1}\left(h\frac{\partial\bar{\psi}^e}{\partial z}\right) \Rightarrow \bar{\bar{r}}^h\bar{\bar{D}}\bar{\bar{r}}^e\bar{\phi}^e = \bar{\bar{D}}_z\bar{\phi}^e$$
$$\bar{\bar{r}}^{e-1}\left(h\frac{\partial\bar{\psi}^h}{\partial z}\right) \Rightarrow -\bar{\bar{r}}^e\bar{\bar{D}}^t\bar{\bar{r}}^h\bar{\phi}^h = -\bar{\bar{D}}_z^t\bar{\phi}^h \tag{20}$$

where superscript t denotes the transposed matrix and D is the bidiagonal matrix which has been formulated in [13]–[16]. The second derivatives of the potential vectors are transformed to:

$$\bar{\bar{r}}^{e-1}\left(h^2\frac{\partial^2\psi^e}{\partial z^2}\right) \Rightarrow \bar{\bar{D}}_z^t\bar{\bar{D}}_z\bar{\phi}^e = -\bar{\bar{D}}_{zz}^{ee}\bar{\phi}^e$$
$$\bar{\bar{r}}^{h-1}\left(h^2\frac{\partial^2\psi^h}{\partial z^2}\right) \Rightarrow -\bar{\bar{D}}_z\bar{\bar{D}}_z^t\bar{\phi}^h = -\bar{\bar{D}}_{zz}^{hh}\bar{\phi}^h. \tag{21}$$

Note that the unknown voltage reflection coefficient is directly involved with the first element of $\bar{\bar{r}}^e$ and its related matrices.

Helmholtz' equations for ψ^e and ψ^h can now be transformed to uncouple the differential equations in the

space-spectral domain via the complex transformation matrices $\bar{\bar{T}}^{e,h}$, which can be obtained numerically from an eigenvalue analysis [21]:

$$\frac{d^2\bar{V}^e}{dy^2} - \left(\alpha^2 + \frac{\bar{\bar{T}}^{e-1}\bar{\bar{D}}_{zz}^{ee}\bar{\bar{T}}^e}{h^2} - \epsilon_r k_0^2\right)\bar{V}^e = 0$$

$$\frac{d^2\bar{V}^h}{dy^2} - \left(\alpha^2 + \frac{\bar{\bar{T}}^{h-1}\bar{\bar{D}}_{zz}^{hh}\bar{\bar{T}}^h}{h^2} - \epsilon_r k_0^2\right)\bar{V}^h = 0 \quad (22)$$

with

$$\bar{\phi}^{e,h} = \bar{\bar{T}}^{e,h}\bar{V}^{e,h}$$

where α is the Fourier transform factor along the x-direction. As mentioned in [21], sometimes the columns of the complex transformation matrices $\bar{\bar{T}}^{e,h}$ have to be suitably rearranged such that the elementary matrix $\bar{\bar{\delta}} = \bar{\bar{T}}^{h^t}\bar{\bar{D}}_z\bar{\bar{T}}^e$ retains quasi-diagonal properties [13]–[16]. This is usually done by sorting the absolute eigenvalues. It is worthwhile noting that the matrices $\bar{\bar{T}}^{e,h}$ are unique once the longitudinal boundary conditions are given and they are totally independent of the metallic contour of the discontinuity. The conductor circuit is only involved in form of the basis functions which will be explained later. The solution to (22) simply describes the wave propagation in the y-direction and can be written as a set of inhomogeneous transmission line equations which gives a relationship for $\bar{V}^{e,h}$ and its derivatives in the bottom and top boundaries of one dielectric layer [19].

Applying the continuity condition at each dielectric interface leads to a matrix relationship between the tangential field components of two adjacent subregions in the interface plane. Next, by successively utilizing the continuity condition and multiplying the resulting matrices by the transmission line matrices associated with the multilayer subregions, the boundary conditions from the top and bottom walls can be transformed into the interface plane of the discontinuity. This leads to a kind of space-spectral Green's function in the transformed domain which must be transformed back into the original domain [19]. This step can be performed by the conventional MOL and SDA procedures independently. From the mathematical viewpoint there is no difference which procedure is applied first. However, applying the MOL first leads to a better physical understanding and easier mathematical treatment. Since the planar conductors continuously extend over the entire surface of the circuit, the discretization lines intersecting the conductor section are equal to the total number ($2 \times k$) of the potential lines. As a result, the matrix elements of the resulting Green's function in the space-spectral domain are once again coupled to each other through the reverse transformation back into the original domain:

$$\begin{pmatrix} \bar{\bar{Z}}_{xx}(\alpha) & \bar{\bar{Z}}_{xz}(\alpha) \\ \bar{\bar{Z}}_{zx}(\alpha) & \bar{\bar{Z}}_{zz}(\alpha) \end{pmatrix} \begin{pmatrix} \bar{i}_x(\alpha) \\ j\bar{i}_z(\alpha) \end{pmatrix} = \begin{pmatrix} \bar{e}_x(\alpha) \\ j\bar{e}_z(\alpha) \end{pmatrix} \quad (23)$$

This equation is now subject to the SDA technique from which the eigensolution can be obtained directly in the spectral domain. To do so, the Galerkin's technique is used together with an appropriate choice of basis functions defined on the conductor surface for each slicing line in the z direction. This leads to a characteristic matrix equation system which must be solved for the zeros of its determinant. Whereby the determinant is a function of the reflection coefficient r:

$$\bar{\bar{F}}(r)\begin{bmatrix} \bar{a} \\ \bar{b} \end{bmatrix} = 0. \quad (24)$$

In contrast to the 3-D SDA, only one-dimensional basis functions are needed here. In order to achieve a fast algorithm, the following trigonometric functions combined with the edge condition are used:

$$i_{xp}^{m^h}(x) = \frac{a_p^{m^h} \sin\left\{\dfrac{p\pi(x-s)}{w}\right\}}{\sqrt{1 - \left\{\dfrac{2}{w}(x-s) - 1\right\}^2}},$$

$$p = 1, 2, 3, \cdots \text{ with } m^h = 1, 2, \cdots, k$$

$$i_{zq}^{m^e}(x) = \frac{b_q^{m^e} \cos\left\{\dfrac{q\pi(x-s)}{w}\right\}}{\sqrt{1 - \left\{\dfrac{2}{w}(x-s) - 1\right\}^2}},$$

$$q = 0, 1, 2, \cdots \text{ with } m^e = 1, 2, \cdots, k \quad (25)$$

where $a_p^{m^h}$ and $b_q^{m^e}$ denote the unknown modal current coefficients, which must be determined for each line. Note that e and h refer to electric and magnetic potential lines, respectively. Subscripts p and q denote the number of the basis functions. For irregularly shaped discontinuities, the geometric parameters w and s become a function of the z-coordinate and therefore are different for each line. In general, this does not complicate the analysis of planar structures at all, as long as the circuit contour can be described mathematically or by a set of coordinates. It should be emphasized that, due to the flexibility in handling arbitrary circuit topology, the SSDA is very well suited for contour-driven CAD software. In addition, singularities of the circuit in the x direction are automatically considered in the formulation of the basis functions.

Once the voltage reflection coefficient r (s_{11}) is known, an arbitrary constant for the first element of the x-oriented current coefficients can be assumed. Applying a singular value decomposition technique to (24) yields all the current coefficients for the chosen basis functions assigned to each discrete line. Therefore, the total surface current across the line can be obtained by a simple integration. It is worthwhile pointing out that infinite summation of the spectral terms, when constructing the characteristic equation $\bar{\bar{F}}$ in (24) must be truncated at a suitable value N for

practical calculations. N can be different for each line. However, for simplicity, only equal numbers for each line will be considered in the following calculations.

Results and Discussion

First of all, the influence of the voltage reflection coefficient $r(s_{11})$ on the error function is examined by assuming that the 3 dB criterion defined in (15) and (16) is satisfied for two cases: $h/\lambda_g = 0.2$ and $h/\lambda_g = 0.05$. It is important to note that such a function is related only to the discretization error and cannot be regarded as the overall accuracy criterion although both errors are related to each other to some extent. Fig. 2 and Fig. 3 display the magnitude of the error function versus the phase of s_{11} in degrees at Port 1 which varies from 0° to 360° with different voltage reflection coefficients. It is obvious that choosing a fine discretization significantly reduces the error term. On the other hand, maximum and minimum error may occur at different locations of the phase. In case of $h/\lambda_g = 0.05$, for example, maximum error points are quasi-symmetrically located at two sides of one minimum location around $\angle s_{11} = 175°$ while in case of $h/\lambda_g = 0.2$ two minimum locations exist which are close to $\angle s_{11} = 160°$ and $\angle s_{11} = 320°$, respectively. Another observation is that the error for small reflections appears to be smaller than that of larger reflections, which can be explained by the fact that a higher reflection yields a distinct variation of the standing-wave pattern and consequently causes higher discretization error of the differential operators. This is in particular true if the reference plane of discretization coincides with the position on the line where a strong variation of the waveform occurs. In other words, choosing different lengths of the feed line and/or terminal line results in different phase terms of the voltage reflection coefficient at the reference plane with no change in the magnitude of r.

To demonstrate the SSDA, three simple examples of through-lines with matched, open- and short-circuit conditions at the boundary of Port 2 are given. Since only propagation of the fundamental mode is considered along the uniform transmission lines, one basis function of each J_x and J_z component is needed to provide enough accuracy. Fig. 4 shows a convergence test of $\angle s_{11}$ for a short-circuited through microstrip line as a function of the truncated spectral term along the x-direction with different discretization size. It can be seen that the convergence is quite beyond $N = 75$ for three discretization sizes.

Fig. 5 displays the surface current distribution of J_x and J_z components along the longitudinal direction of the line under matched condition. There is a negligible standing-wave ($|r| = 0.022$) on the line which should not be the case if the matching were perfect. This phenomenon can be explained by the fact that the matched condition implemented in this theory is a necessary condition which does not provide a complete match due to the error of discretization and the truncated terms of the infinite spectrum. This has also been reported in [24]. Increasing the spectral term N can improve the mismatch (i.e., $|s_{11}| = 0.059$ for $N = 100$ to 0.022 for $N = 150$). In addition, the magnitude of J_x tends to vanish because of its anti-symmetry of the current distribution on the conductor.

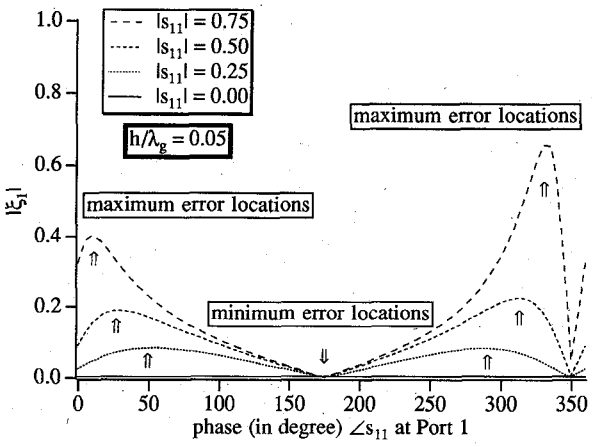

Fig. 2. Magnitude of the error function at Port 1 as a function of the angle of r with different magnitudes of r in case of fine discretization.

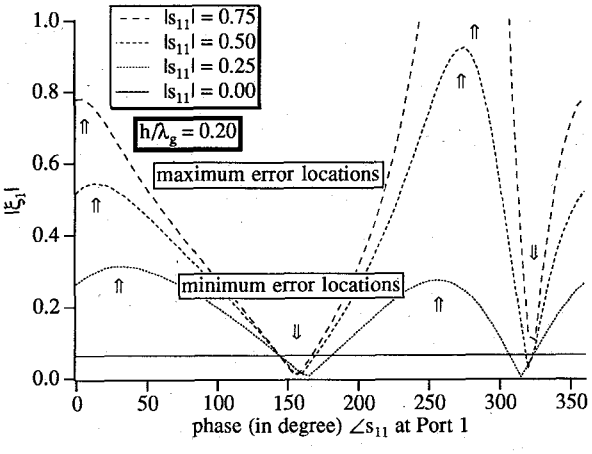

Fig. 3. Magnitude of the error function at Port 1 as a function of the angle of r with different magnitudes of r in case of rough discretization.

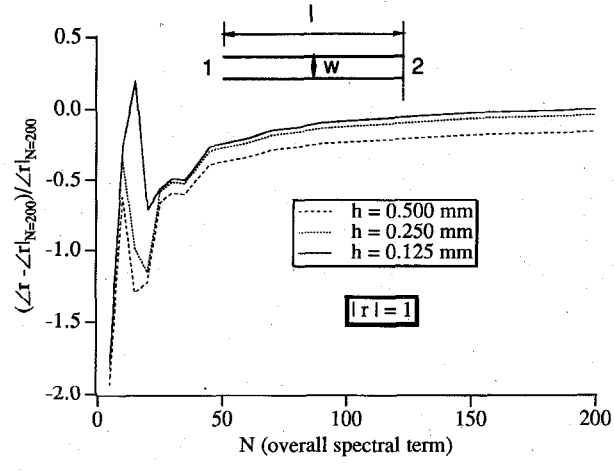

Fig. 4. Relative convergence behavior of the voltage reflection coefficient $\angle r$ versus the truncated spectral term N with different discretization size for a shorted through microstrip line. $|r| = 1$ is always obtained. The parameters used in the calculation: $l = 9$ mm, $w = 1$ mm, $h = 0.25$ mm, $a = 10$ mm, $s = 4.5$ mm, $f = 12$ GHz, $\epsilon_r = 10$, $\epsilon_{eff} = 8.0474$ and substrate thickness is 0.25 mm.

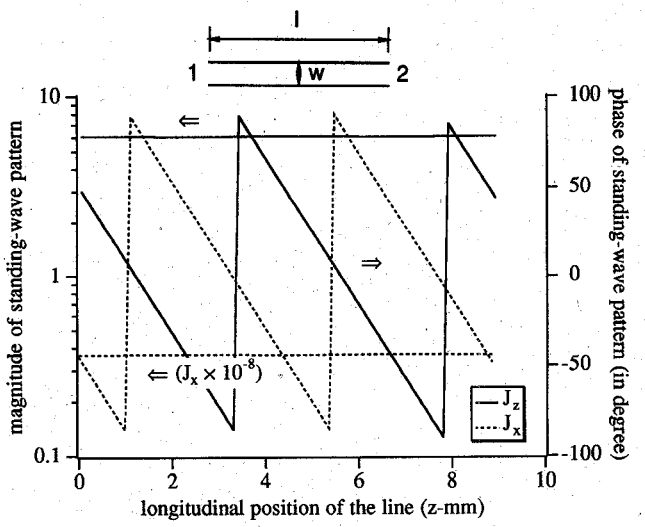

Fig. 5. Magnitude and phase distributions along the z-direction of the through microstrip line as described in Fig. 4 with the matched condition.

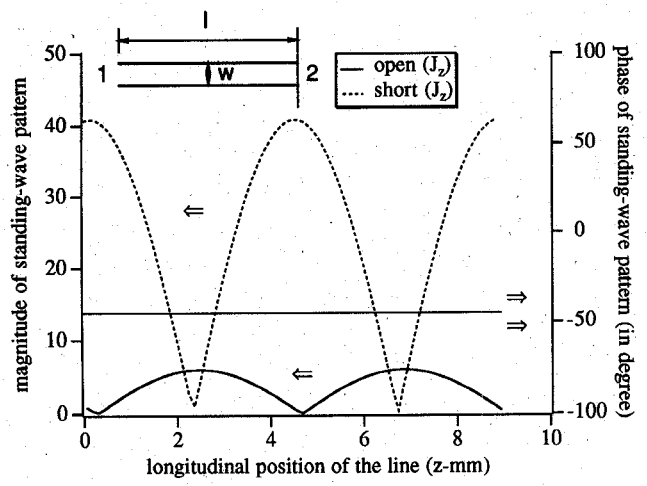

Fig. 6. Standing-wave profiles of the J_z component along the through microstrip line as described in Fig. 4 with the short and open-circuit termination.

Fig. 6 illustrates the complete standing-wave of the J_z component along the line with the open and short at Port 2 ($|r|$ at $z = 0$ is 1.0 for both open and short circuits), which agrees well with the physical perception. As expected, the maximum and minimum points for the open and short are alternatively located, and the open and short points of the line are clearly indicated by the magnitude of the standing-waves.

Fig. 7 shows a comparison of the parameter s_{11} obtained by this method and by others (i.e. [21], [25]) for a microstrip step discontinuity. A good agreeent can be observed over the frequency range up to 25 GHz, while a small discrepancy of numerical results appears beyond that frequency range. This may be due to different dimensions of the shielding box.

Transmission characteristics of two closely spaced microstrip step discontinuities are shown in Fig. 8. It is evident that there is a strong interaction between both steps since the separation of both steps is less than half the

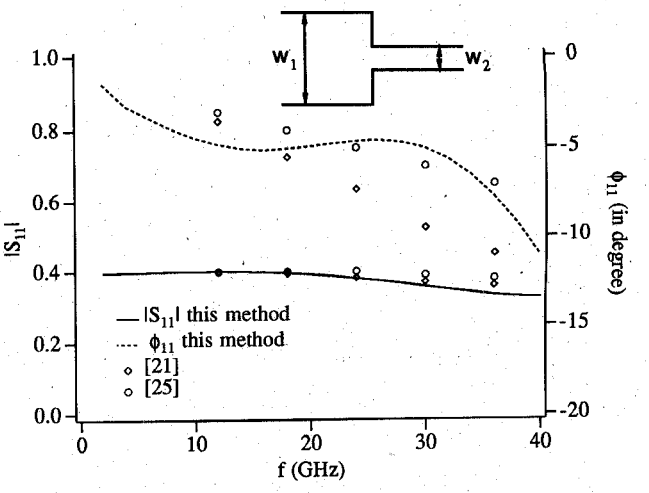

Fig. 7. Frequency-dependent reflection characteristics (s_{11}) of a microstrip step discontinuity. $w_1 = 1.00$ mm, $w_2 = 0.25$ mm, $\epsilon_r = 10.0$, $a = 10$ mm and thickness of the dielectric substrate $t = 0.25$ mm.

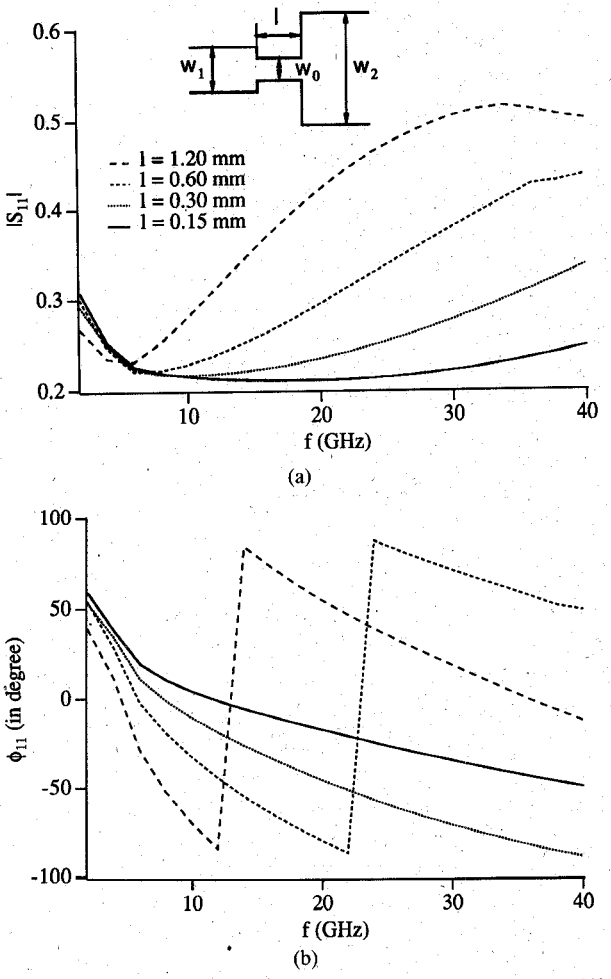

Fig. 8. S-parameters for a cascaded step discontinuity separated by a transmission line of length l. $w_1 = 0.4$ mm, $w_0 = 0.2$ mm, $w_2 = 0.8$ mm, $\epsilon_r = 3.8$, $a = 5$ mm and $t = 0.25$ mm. (a) Magnitude of s_{11}. (b) Phase of s_{11}.

guided wavelength. Interestingly, a tighter coupling of both steps leads to a lower reflection coefficient over the frequency. The phase of the step discontinuity is shown in Fig. 8(b). These results suggest that a strong inter-

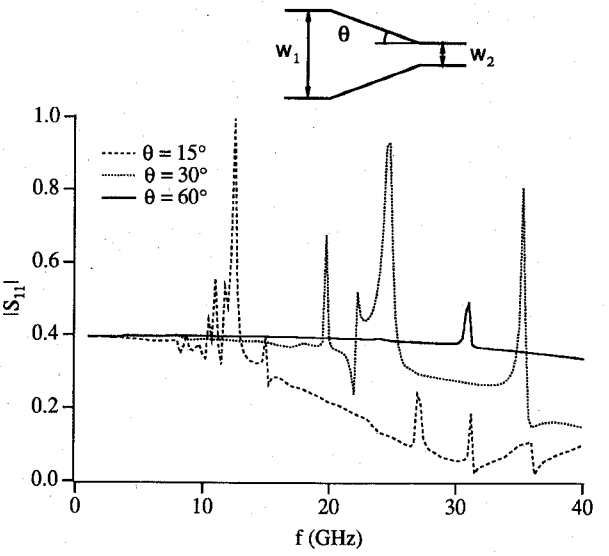

Fig. 9. Frequency response of a linear taper with a variable angle θ. Dimension of the structure is the same as that used in Fig. 7.

action between two single step discontinuities is not limited to only cases of short interconnecting stubs.

The frequency-dependent reflection characteristic of a linear microstrip taper is presented in Fig. 9 to demonstrate the flexibility and efficiency of this full-wave approach when arbitrary discontinuity contours are considered. The limiting case of the taper is $\theta = 90$ degree in which the taper is reduced to an abrupt step discontinuity analyzed in Fig. 7. An oscillating behavior of s_{11} appears in cases of long tapers ($\theta = 30$ degree and $\theta = 15$ degree) which indicates some kind of resonance effect. For the $\theta = 15$ degree taper this resonance effect occurs at higher frequencies than for the one with $\theta = 30$ degree. Similar characteristics of linear microstrip tapers have been obtained by the planar circuit approach in [26].

Conclusion

A new approach using the Space-Spectral Domain Approach (SSDA) has been presented to calculate scattering parameters and field/current distributions for three-dimensional discontinuity problems in MIC/MMIC circuits. The theory presented in this paper demonstrates how to implement self-consistent hybrid boundary conditions. Analytical error functions are introduced for the first time to estimate the error magnitude due to the discretization scheme used in this method. The convergence behavior of the method is illustrated as a function of the truncated spectral terms and with different discretization sizes. Surface current standing-wave profiles along microstrip through-lines with matched, open- and short-circuit conditions are calculated. A comparison with results from other methods validates this new approach. Some practical discontinuities including the linear microstrip taper have been analyzed, to demonstrate the efficiency and flexibility of this technique in treating arbitrary planar circuit contours frequently found in M(H)MIC's.

References

[1] K. S. Yee, "Numerical solution of initial boundary value problems involving Maxwell's equations in isotropic media," *IEEE Trans. Antennas Propagat.*, vol. AP-14, pp. 302–307, May 1966.

[2] X. Zhang and K. K. Mei, "Time-domain finite difference approach to the calculation of the frequency-dependent characteristics of microstrip discontinuities," *IEEE Trans. Microwave Theory Tech.*, vol. 36, pp. 1775–1785, Dec. 1988.

[3] S. Akhtarzad and P. B. Johns, "Three-dimensional transmission-line matrix computer analysis of microstrip resonators," *IEEE Trans. Microwave Theory Tech.*, vol. MTT-23, pp. 990–997, Dec. 1975.

[4] W. J. R. Hoefer, "The transmission-line matrix method—theory and applications," *IEEE Trans. Microwave Theory Tech.*, vol. MTT-33, pp. 882–893, Oct. 1985.

[5] R. W. Jackson, "Full wave finite element analysis of irregular microstrip discontinuities," *IEEE Trans. Microwave Theory Tech.*, vol. 37, pp. 81–89, Jan. 1989.

[6] J. C. Rautio and R. F. Harrington, "An electromagnetic time-harmonic analysis of shielded microstrip circuits," *IEEE Trans. Microwave Theory Tech.*, vol. MTT-35, pp. 726–730, Aug. 1987.

[7] T. Itoh and R. Mittra, "A technique for computing dispersion characteristics of shielded microstrip lines," *IEEE Trans. Microwave Theory Tech.*, vol. MTT-21, pp. 896–989, Oct. 1976.

[8] R. H. Jansen, "The spectral domain approach for microwave integrated circuits," *IEEE Trans. Microwave Theory Tech.*, vol. MTT-33, pp. 1043–1056, 1985.

[9] M. Helard, J. Citerne, O. Picon, and V. F. Hanna, "Theoretical and experimental investigation of finline discontinuities," *IEEE Trans. Microwave Theory Tech.*, vol. MTT-33, pp. 994–1003, Oct. 1985.

[10] W. Wertgen and R. H. Jansen, "Iterative, monotonically convergent hybrid mode simulation of complex, multiply branched (M)MIC conductor geometries," in *1990 IEEE MTT-S Int. Microwave Symposium Dig.*, pp. 559–562.

[11] R. Sorrentino and T. Itoh, "Transverse resonance analysis of finline discontinuities," *IEEE Trans. Microwave Theory Tech.*, vol. MTT-32, pp. 1632–1638, Dec. 1984.

[12] I. Wolff, G. Kompa and R. Mehran, "Calculation method for microstrip discontinuities and T-junctions," *Electron. Lett.*, vol. 8, pp. 177–179, Apr. 1972.

[13] U. Schulz and R. Pregla, "A new technique for the analysis of the dispersion characteristics of planar waveguides," *Arch. Elek. Ubertragung., Band 34*, pp. 169–173, 1980.

[14] S. B. Worm and R. Pregla, "Hybrid mode analysis of arbitrarily shaped planar microwave structures by the method of lines," *IEEE Trans. Microwave Theory Tech.*, vol. MTT-32, pp. 191–196, Feb. 1984.

[15] R. Pregla and W. Pascher, "The method of lines," in *Numerical Techniques for Microwave and Millimeter Wave Passive Structures*, ch. 6, T. Itoh, Ed., New York: Wiley, 1989, pp. 381–446.

[16] K. Wu and R. Vahldieck, "Comprehensive MoL analysis of a class of semiconductor-based transmission lines suitable for microwave and optoelectronic application," *Int. J. of Numerical Modelling*, Special Issue, T. Itoh Ed., vol. 4, New York: Wiley, 1991, pp. 45–62.

[17] H. Diestel and S. B. Worm, "Analysis of hybrid field problems by the method of lines with nonequidistant discretization," *IEEE Trans. Microwave Theory Tech.*, vol. MTT-32, pp. 633–638, June 1984.

[18] K. Wu and R. Vahldieck, "A novel space-spectral domain approach and its application to three-dimensional MIC/MMIC circuits," in *Proc. 19th EuMC*, London, Sept. 1989, pp. 751–756.

[19] ——, "A new method of modeling three-dimensional MIC/MMIC circuits: the Space-Spectral Domain Approach," *IEEE Trans. Microwave Theory Tech.*, vol. 38, pp. 1309–1318, Sept. 1990.

[20] R. W. Jackson, "Full wave, finite element analysis of irregular microstrip discontinuities," *IEEE Trans. Microwave Theory Tech.*, vol. 37, pp. 81–89, Jan. 1989.

[21] Z. Q. Chen and B. X. Gao, "Deterministic approach to full-wave analysis of discontinuities in MIC's using the method of lines," *IEEE Trans. Microwave Theory Tech.*, vol. 37, pp. 606–611, Mar. 1989.

[22] S. B. Worm, "Full-wave analysis of discontinuities in planar waveguides by the method of lines using a source approach," *IEEE Trans. Microwave Theory Tech.*, vol. 38, pp. 1510–1514, Oct. 1990.

[23] T. Uwano and T. Itoh, "Spectral domain approach," in *Numerical Techniques for Microwave and Millimeter Wave Passive Structures*, ch. 5, T. Itoh, Ed., New York: Wiley, 1989, pp. 334–380.

[24] M. Drissi, V. Fouad Hanna, and J. Citerne, "Theoretical and exper-

imental investigation of open microstrip gap discontinuity," in *Proc. 18th EuMC* Sept. 1988, pp. 203–209.
[25] N. H. L. Koster and R. H. Jansen, "The microstrip step discontinuity: a revised description," *IEEE Trans. Microwave Theory Tech.*, vol. MTT-34, pp. 213–223, Feb. 1986.
[26] R. Chadha and K. C. Gupta, "Compensation of discontinuities in planar transmission lines," in *1982 IEEE MTT-S Int. Microwave Symposium Dig.*, pp. 308–310.
[27] W. J. R. Hoefer, "A contour formula for compensated microstrip steps and open ends," in *IEEE MTT-S Int. Microwave Symp. Dig.*, Boston, 1983, pp. 524–526.
[28] D. Raicu, "Universal taper for compensation of step discontinuities in microstrip lines," *IEEE Microwave Guided Wave Lett.*, vol. 1, pp. 249–251, 1991.

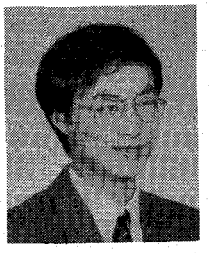

Ke Wu (M'87) was born in Jiangsu, China, on December 9, 1962. He received the B.Sc. degree (with distinction) in radio engineering from Nanjing Institute of Technology, Nanjing, China, in 1982 and the D.E.A. degree in electronics and Ph.D. degree (with distinction) in optics, optoelectronics, and microwave engineering from the Institut National Polytechnique de Grenoble (INPG), Grenoble, France, in 1984 and 1987, respectively.

During the years 1983–1987, he conducted research in the Laboratoire d'Eléctromagnetisme, Microondes et Optoélectronics (LEMO), Grenoble, France. From March 1988 to January 1992 he was a research associate in the Department of Electrical and Computer Engineering at the University of Victoria, Victoria, B.C., Canada. In February 1992, he joined the Département de génie électrique et de génie informatique at the École Polytechnique de Montréal as an assistant professor. His main research interests include electromagnetic fields, numerical methods, analysis and design of various microwave/millimeter-wave integrated and monolithic circuits, planar antennas and microwave/optical signal processing. He is also interested in research and design of broadband optoelectronic components and lightwave transmission systems with emphasis on travelling-wave electro-optic modulators, couplers and switches.

Dr. Wu received a Chinese Overseas Graduate Fellowship in 1982, a U.R.S.I. Young Scientist Award in 1987, and, together with two coauthors, the Oliver Lodge Premium from the IEE for the outstanding publication in 1988.

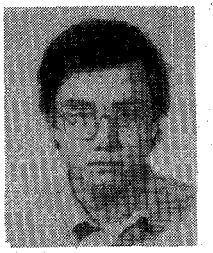

Ming Yu (S'90) was born in Beijing, China in 1962. He received electrical engineering B.S. (with honour) and M.S. from Tsinghua University, Beijing in 1985 and 1986, respectively.

From 1985 to 1989, he worked with Tsinghua University as a research and teaching assistant. From 1989 to 1990, he worked with Beijing CHOFU (Electronics) Co. Since May 1990, he has been working towards his Ph.D. at University of Victoria, Victoria, BC, Canada. His research activities include MMIC's and MHMIC's CAD and measurement, numerical techniques, time-domain EM scattering and imaging, and microwave filter design.

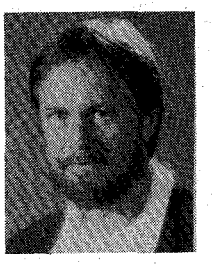

Rüdiger Vahldieck (M'85–SM'86) received the Dipl.-Ing. and the Dr.-Ing. degrees in electrical engineering from the University of Bremen, West Germany, in 1980 and 1983, respectively.

From 1984 to 1986 he was a Research Associate at the University of Ottawa, Canada. In 1986 he joined the University of Victoria, BC, Canada, where he is now a Full-Professor in the Department of Electrical and Computer Engineering. His research interest include numerical methods to model electromagnetic fields for computer-aided design of microwave, millimeter wave and opto-electronic integrated circuits. He is interested in design aspects of passive and active planar and quasi-planar components and filters for MMIC and MHMIC applications. Recently he has been involved in research on subcarrier multiplexed lightwave systems. The emphasis of this work is on broad bandwidth electro-optic modulators and on coherent detection systems in fiber-optic communication links.

Dr. Vahldieck, together with three coauthors, received the outstanding publication award of the Institution of Electronic and Radio Engineers in 1983. He is on the editorial board of the IEEE TRANSACTIONS ON MICROWAVE THEORY AND TECHNIQUES and he has published more than 70 technical papers in the field of microwave CAD.